

An Empirical Study on Generic Multicopter Energy Consumption Profiles

Thomas Dietrich*, Silvia Krug[†] and Armin Zimmermann*

*Systems and Software Engineering Group, Technische Universität Ilmenau, Germany

{thomas.dietrich, armin.zimmermann}@tu-ilmenau.de

[†]Communication Networks Group, Technische Universität Ilmenau, Germany

silvia.krug@tu-ilmenau.de

Abstract—Unmanned Micro-aerial vehicles (MAVs) enjoy high popularity in various application fields. They are capable of flying autonomously, following the instructions received from a controlling ground entity. One physical limitation of all mobile robotic vehicles is the restricted energy storage capacity they are able to carry. All processes in a robotic system, prominently in-air movements, consume energy and are thereby defining the overall operation time limit. This paper presents results of an analysis of the energy consumption in various discrete movement states of a multicopter, measured for two different systems. Findings regarding a systematic relation between system and movement parameters and the energy consumption levels are discussed. Furthermore, a generic energy consumption profile model is presented and validated.

Index Terms—Multicopter Systems; Energy Profiling; Consumption Prediction; Measurements.

I. INTRODUCTION AND RELATED WORK

Micro-Aerial Vehicles (MAVs), especially multicopter systems, are used in many application fields. A prominent use case is to reach inaccessible areas autonomously, for example in reconnaissance missions [1]. In commercial applications the fields of surveillance, photography and transportation of goods or data are greatly interested in multicopter utilization. One multicopter has the size and power to carry and use sensors, cameras or actuators to fulfill a wide variety of tasks. Acquirable sensor data includes images and video, environmental measurements, and other types of data acquired from the exploration area.

Due to the compact form factor, the high maneuverability and the hovering capabilities of multicopters, these are especially useful for the mentioned use cases. Configurations vary in the nature and constellation of wings, motors and propellers, which in return have an influence on the usage capabilities. All mentioned factors have a significant effect on the rather high energy consumption of these mobile robots.

Energy consumption is an important topic in the research field of aerial vehicles because of obvious on-board energy storage constraints. The size- and weight-limited battery of a multicopter provides only a limited energy capacity, which results in a limitation of both overall flight time and flight distance. These can be marginally improved by optimizing both the multicopter hardware setup and the flight and mission planning algorithms. Lightweight construction design can be used to reduce the needed ascension force and energy can be

generated on-board. Solar energy extraction was implemented by [2] in a glider wing configuration to cover the much less energy budget. Another approach to increase overall flight time is to optimize the flight path between predefined positions. In [3] the authors describe a flight planing algorithm to calculate the minimum-energy path by taking the efficiency of angular accelerations in consideration. A similar approach was taken by [4] by optimum path calculation using the Dijkstra Algorithm.

None of the presented solutions is fully able to eliminate the need for recharging or battery replacement. Therefore, additional research was done in the area of energy aware mission planning. In [5] an autonomous hardware system for instantaneous battery replacement was presented. An approach with autonomous battery recharging, including a swarm-aware scheduling algorithm is described in [6]. A theoretical power and endurance model was discussed and tested by [7] with the focus on weight efficiency and optimal battery selection. An extension of an existing and widely implemented communication protocol for MAVs was extended by swarm related energy maintenance tasks and presented in [8].

The contribution of this paper are systematic multicopter flight experiments, the statistical analysis of energy usage patterns, and the derivation and validation of empirical formulas to estimate power consumption (and thus remaining flight time or the ability to complete an upcoming task) of multicopter UAVs. Such insights are necessary for higher-level mission planning and the decision to call back a multicopter for recharging, or an optimal assignment of copters to tasks in a swarm setup.

The remainder of the paper is organized as follows: First, we will introduce the measurement setup of our empirical study in section II. Section III briefly covers the background of this study and the theory behind the measurement analysis and present details on the statistical approach, the calculation of the power consumption, and finally presents the derived energy profile. In section IV findings in regard to the power consumption in general and in relation to influencing factors is shown and a simple energy consumption prediction is carried out to validate the results. Finally, conclusions are given.

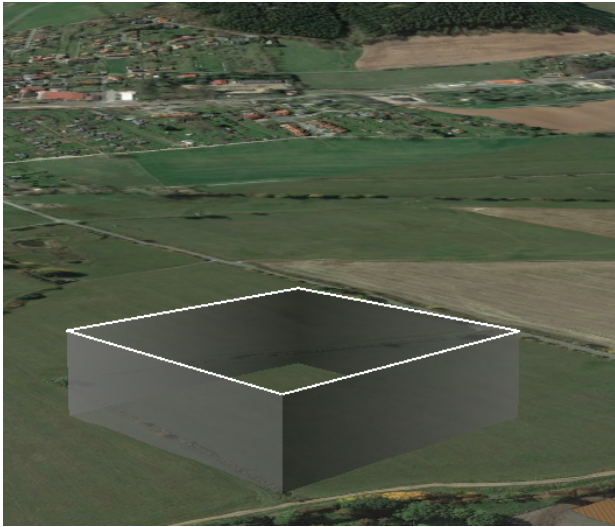


Fig. 1. Benchmark #2 - Squared Flight Pattern

II. MEASUREMENT SETUP

To perform empirical evaluation we used two different multicopter systems. The first one is a commercial Solo quadcopter by 3D Robotics [9], which is used as a reference platform to other commercial products. The second is a non-commercial quadcopter that has been custom-built from common off-the-shelf components. This copter is used for comparison and validation measurements to retrieve more generic insights on flight phase energy consumption in general.

Both quadcopters are based on the same microcontroller and are equipped with the *ArduCopter* firmware [10] tailored to each system to enable autonomous flights. This setup provides the same flight algorithms for both systems. The mission planning for each autonomous flight is done inside the *Mission Planner* PC software [11].

In order to evaluate the actual energy consumption of various flight phases, we planned multiple missions, each featuring different aspects and flight maneuvers. After first test flights with different combinations we identified three configurations as benchmarks for our energy profiling later on. These configurations reflect the major components of multicopter movements: the energy needed to maintain the current altitude, the energy needed for horizontal movement and finally the energy needed for movements with vertical components.

A simple mission is used to obtain a value for the energy

TABLE I
UTILIZED MULTICOPTER SYSTEMS

	3DR Solo	Custom Build
Weight	1800 g	1150 g
Bat. Voltage	14.8 V	11.1 V
Bat. Capacity	5200 mA h	2200 mA h

consumption in hover mode. To achieve this, the copter is flying to a given position and stays there for about 10 min, holding the position at the configured altitude. For this experiment we chose a flight area with almost no wind in order to avoid any influence of horizontal repositioning due to windy conditions. To obtain measurement values for horizontal position change irrespective of any wind influences, we decided to use a squared flight pattern which is sketched in Figure 1. In this pattern, the quadcopter is flying from waypoint to waypoint on a straight line without changing its altitude, until the square is completed and the quadcopter returns to its initial position. This setup ensures that the impact of wind from any given direction could be averaged out as it constantly affects each flight phase from a different angle. Finally, the vertical position change is evaluated using a mission where the quadcopter repeatedly flies from its current altitude to another position with a higher altitude at a given climb angle as shown in Figure 2. After reaching the position, the quadcopter flies to the next position with its original altitude in order to capture the same angle but for declining movements. This flight pattern is repeated multiple times allowing measurements for different climb angles.

For each flight pattern in the different missions we planned a certain minimum flight duration by choosing appropriate positions. This ensures that we gather enough individual measurements for our statistical analysis of the different flight phases. Based on this general concept, we performed multiple flights with each quadcopter for each setup. In total, we performed 6-7 flights of each mission and thus also the respective flight patterns.

Since both systems use the same firmware, they show similar flight characteristics even so the individual flight parameters are different. One important thing to note is, that whenever a quadcopter switches from one flight phase to the next at a given waypoint, there is some transient behavior resulting in slight deviations in flight characteristics. This has

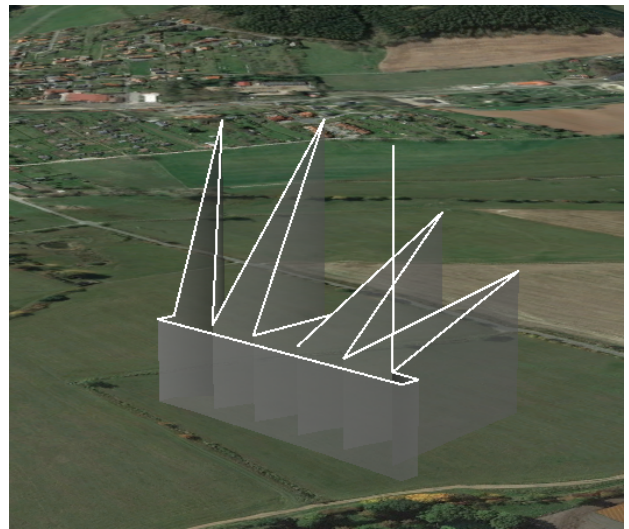


Fig. 2. Benchmark #3 - Climb/Decline Flight Pattern

been taken into account in the statistical analysis described below. It should also be noted, that we did not vary the internal flight parameters, e.g. speed control parameters, during the measurement flights.

The ArduCopter firmware collects very detailed logging information throughout a flight. Information regarding the flight control, mission execution, GPS readings, battery depletion and more is sampled every 100ms. The created log files can be retrieved from the internal flight controller memory after flight and are in comma separated values file format.

III. BACKGROUND AND THEORY

The goal of this empirical analysis is the creation of an energy consumption profile for an unknown multicopter. The characterization of this de facto black box system should be based on real-world observations and on the general principles of multicopters as described below. Other than with theoretical models based on mechanical, electro technical or aerodynamic properties of one system, this work concentrates on providing a reliable energy consumption profile only by the help of empirical data and correlations found between these and mission parameters.

In the context of this research, a mission should be defined as a combination of either hovering or point-to-point maneuvers. Hovering is characterized by a fixed position in air and a duration. A point-to-point maneuver is represented by two points and a straight movement between them. Missions are planned ahead and are executed by the flight controller of the multicopter.

The complex multicopter system can be represented as a simple model considering only its energy consumption over the course of a mission. A small fixed-weight object invests electrical energy to allow controlled movement above ground in all directions. Due to the gravitational force, a certain amount of energy is always needed to hold the multicopter in air. Additionally, changes in its position will have a negative or positive impact on the energy consumption. The simplified multicopter model is depicted in Figure 3. The horizontal movement direction of the multicopter can be safely ignored because of both the adjustable heading and the high symmetry of the multicopter.

The movement speed along a point-to-point maneuver is chosen by the control loop based on the movement direction and will have a reasonable impact on energy consumption. Parameters controlling speed decisions are set inside the flight control and can not be changed over the course of one mission.

Based on these simplifications, the overall energy consumption of an unknown multicopter can be divided into two parts: First, the energy needed to hold the multicopter in its position (hover, force F_G), and second the energy needed to change the position along a movement vector (\vec{s}). Significant factors defining the hovering energy part are multicopter build specifics like number of and efficiency of the motors, material and quality of the propellers, and total weight. These properties are assumed to be constant for a multicopter system, a realistic assumption at least during one flight.

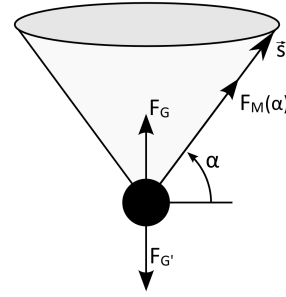


Fig. 3. Abstract Multicopter Model in the Discussed Context

Flying along a movement vector defines the second part of the overall energy consumption. A movement vector characterizes either a horizontal and vertical displacement or the direction and the speed of a movement. Because of the mentioned unbounded horizontal freedom of movement of a multicopter, its climb or decline angle α can be extracted as the relevant part of the movement vector direction. The mentioned forces and the movement in any direction at a certain angle are presented in Figure 3.

First observations do show clear relations between the movement angle and the movement speed chosen by the flight controller.

In conclusion, only the flight angle as one variable factor is expected to have a measurable impact on the energy consumption for one multicopter over the course of one mission in the previously described measurement setup, resulting in the dependency $F_M(\alpha)$. Furthermore, relevant invariant factors changeable in-between flights are the total weight and the speed parameterization of the flight control. Modifications to the multicopter setup, such as the materials and components used or values of other control parameters, not considered here as they would usually require a new calibration of the model. These mentioned factors are not in the scope of this work. Wind is one other factor of influence on the energy consumption, which is not part of this research and was negligible during all measurement flights.

A. Statistical Analysis

The detailed analysis of all measurements was performed in the statistical computing language R. In total, 20 individual captured flights have been selected. This includes log files from both multicopter systems and of all described flight variations. The developed R analysis script¹ consists of the following steps.

Each log file is loaded into memory and parsed for relevant data. All data entries consist of a timestamp and fine grained discretized sampling data for different relevant aspects of the covered data types. These include system status data, mission commands/waypoints, GPS data and raw consumption measurement data, besides others.

The first step in further computation is the selection of individual maneuvers and their steady states in-between tran-

¹available online at <https://github.com/tuiSSE/ardupilot-energy-analysis>

IV. RESULT AND VALIDATION

A. Measured Power Consumption

The measurements and examinations were done with the Solo quadcopter in general and with the described custom build copter for comparison. Results of the 10 min hover benchmark described in Section II executed with the Solo quadcopter are shown as a histogram of sampled power readings in Figure 5. The power consumption during the steady-state of hovering is approximately normally distributed with parameters

$$\mu = 262.7 W \quad \sigma = 5.2 W \quad (1)$$

To evaluate these numbers a comparison was carried out with the internally summed up energy consumed by the system. Over a steady hover flight time of 8 min 48 s the multicopter consumed 37.46 Wh. Using the results from above, the following energy consumption is expected:

$$\begin{aligned} E_{el} &= \mathcal{N}(262.7, 5.2^2) W \cdot 528 \text{ sec} / 3600 \text{ sec} \\ &= \mathcal{N}(38.43, 0.76^2) Wh \end{aligned} \quad (2)$$

A z-score of -1.27σ between these different sources of data is well inside the expectable inaccuracy of the sampled readings as well as of the computational steps in between. The close proximity allows further analysis steps based on the measurement samplings.

Mean power consumption while hovering can be seen as an invariant portion of one multicopter's power consumption, which is needed to counterbalance earth's gravitational force. All other movements will have an additional (or decreasing) influence on top of this constant value.

B. Flight Angle Correlation

The climb or decline angle was already named as one of the important influencing movement factors on multicopter energy consumption. Both the square and the angle-oriented benchmark flight missions presented in Section II were executed with the 3DRSolo copter multiple times on different days to get reliable data for angle-consumption correlations. The results in Figure 6 show a clear relation between both.

The mean values of one angle from all flights are in close proximity, standard deviation is approximately equal among all

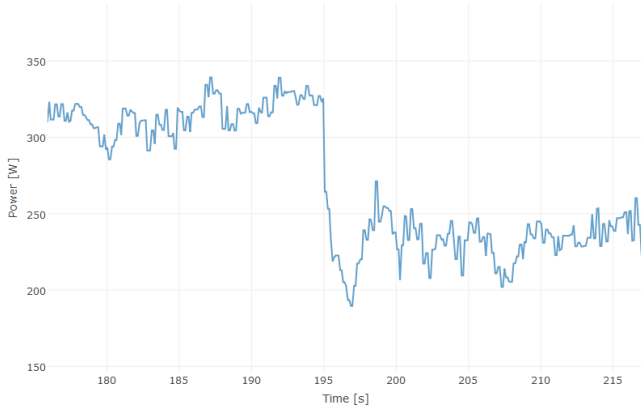


Fig. 4. Maneuver Transition Power Measurements

sitions. Each maneuver is described by the start and end timestamps, the underlying command type and the command ID of both the previous and active command needed to derive the maneuver path. As shown in Figure 4, the transition between two distinct maneuvers is observable as a clear change in mean total power draw for a short duration. Selection of power consumption samples from the flight log is hence done based on the extracted timestamps with a guard band of a few seconds/meters subtracted on both ends of the transition.

Measurements from within these selected regions are statistically analyzed to compute the power draw of the system over the course of one maneuver, represented as mean value and standard deviation. Additionally, the overall consumed energy is calculated. The climb/decline flight angle and the traveled distance along this path are computed from both the predefined maneuver command instructions as well as from the raw GPS recordings for later comparison. The important parameter *speed of flight* can not be extracted from the maneuver commands and was derived from the respective GPS coordinates and the traveling time on the linear path between them. The calculated speeds are expected to be of an acceptably high precision. The reasoning for this is the high HDOP² throughout all measured flights as well as the negligible GPS position error w.r.t. the maneuver distances.

The described computations are done for all maneuvers of one flight and for all selected flights. Each flight was tagged with information and data regarding the general condition of the flight, including surrounding weather conditions, like temperature or wind, weight additions, and hardware setup details. Later analyses based on these influencing factors is thereby possible.

The last part of the statistical analysis concentrates on correlations between different maneuvers based on single parameters. Energy consumption values from all flights and maneuvers are for example compared based on their respective flight angle. Conclusions regarding the more general energy consumption profile can be derived from these considerations.

²Horizontal Dilution Of Precision, GPS 2D precision quality indicator

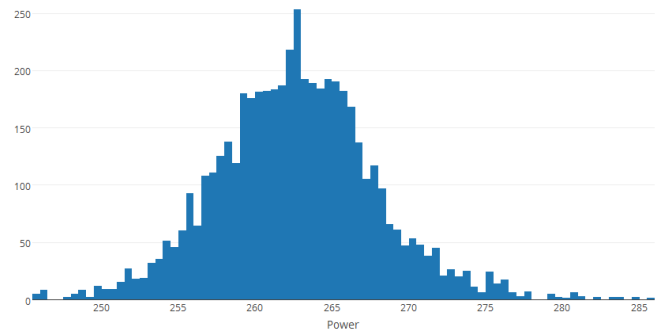


Fig. 5. Hover Power Histogram

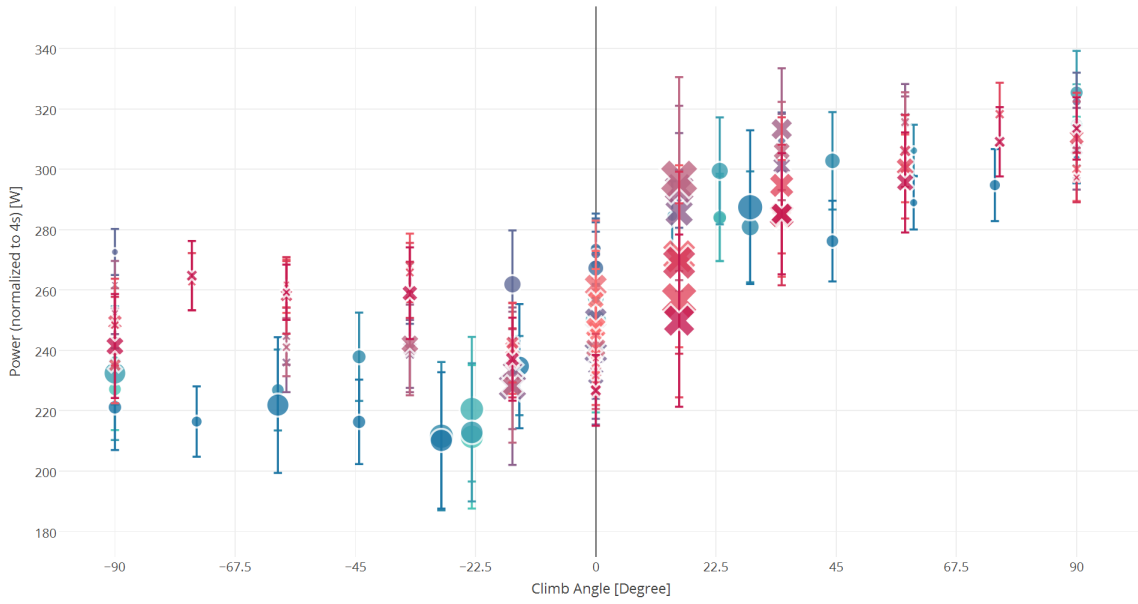


Fig. 6. Power Consumption as $\mathcal{N}(\mu, \sigma^2)$ in Relation to Climb/Decline Angle (Red/Crosses: 3DR Solo Copter – Blue/Circles: Custom Build Copter)

measured maneuvers. It is clearly visible, that more power is drawn at climbing angles than at declining angles, which was expected. Steeper angles, however, did not show a proportional effect on the consumption, contrary to our expectations. In fact, consumption at $\pm 90^\circ$ is even lower than at close-by sloped angles. We see the reason for this behavior in the flight speed being controlled by the flight controller and selected significantly slower apart from 0° : While the 3DR Solo is traveling with 8 m/s at 0° , it is only traveling with 1.2 m/s in a -90° maneuver.

The same missions were executed by the custom build multicopter and the 3DR Solo multicopter for comparison. The measurements taken from the 3DR Solo are presented in Figure 7. Results for both are presented in Figure 6 (Custom build copter values normalized). While absolute values differ slightly, the trend of the results is the same. The observed behavior with regard to climb/decline angle and speed of flight

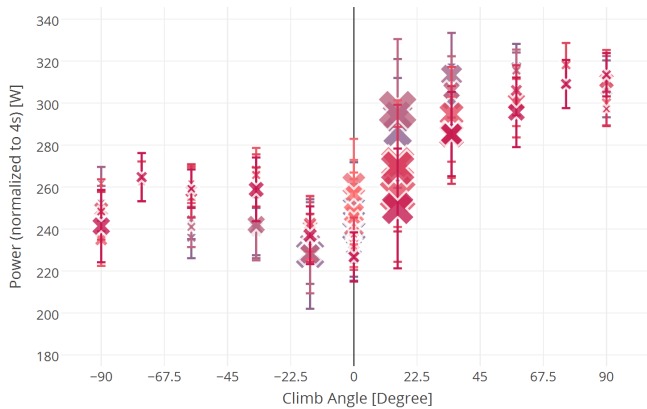


Fig. 7. Power Consumption in Relation to Climb/Decline Angle, 3DR Solo

are nearly identical, and the standard deviation of the power consumption is comparably small. Differences can be seen in the results for declining angles. We assume that among the reasons are differently configured control parameters or construction and material differences.

C. Energy Profile Definition

Based on the values obtained for each flight phase in the previous section, we calculated the energy consumption of different flight phases as well as the total power consumption for the complete flight of the benchmark flights introduced before. These consumptions were then compared to the actual values measured by the quadcopter logs. To predict the energy consumption of a flight maneuver, we use a calculation based on the climb angle α_c and the distance d_c of the given command as specified in the flight planning software. As shown in Equation 3, we are dividing the energy consumed into two parts as discussed before:

- Energy needed to withstand gravitational force: $Q_G(t)$
- Energy needed for movement: $Q_M(\vec{s})$

Both parts are proportional to the time t_c in a given command, the movement is additionally dependent on the movement vector \vec{s} consisting of the command distance d_c and the climb angle α_c . The command execution time is moreover itself dependent on the climb angle, because the speed is chosen by the multicopter based on this parameter.

$$\begin{aligned}
 Q_{pred} &= Q_G(t) + Q_M(\vec{s}) \\
 &\Downarrow \\
 Q_{pred} &= Q_G(t_c) + Q_M(\alpha_c, d_c)
 \end{aligned} \tag{3}$$

By applying the known relations $Q = I \cdot t$ and $t = d/v$, this general formula can be transformed for the previously mentioned fundamental flight maneuvers:

V. CONCLUSION AND FUTURE WORK

We have shown which aspects of a multicopter mission significantly influence its power consumption, and proposed an empirical prediction formula. Power readings from multiple flights and different scenarios were analyzed in a systematic study with black box multicopter systems in real-world experiments. Systematic behavior has been identified and correlations between different flight parameters and an approximately normally distributed power consumption was discovered. The formula was validated by predicting the needed energy for two missions with acceptable deviations.

The insights gathered through this empirical study will be the basis for further research in the field of energy consumption prediction in autonomous missions, which is especially important for the coordination of replacement and recharging maintenance maneuvers.

ACKNOWLEDGMENT

This work was supported by the Federal Ministry for Education and Research of Germany [01S13031A].

REFERENCES

- [1] A. C. Watts, V. G. Ambrosia, and E. A. Hinkley, "Unmanned aircraft systems in remote sensing and scientific research: Classification and considerations of use," *Remote Sensing*, vol. 4, no. 6, pp. 1671–1692, 2012. [Online]. Available: <http://www.mdpi.com/2072-4292/4/6/1671>
- [2] S. Morton, R. D'Sa, and N. Papanikolopoulos, "Solar powered UAV: Design and experiments," in *Intelligent Robots and Systems (IROS), 2015 IEEE/RSJ International Conference on*, Sept 2015, pp. 2460–2466.
- [3] F. Morbidi, R. Cano, and D. Lara, "Minimum-energy path generation for a quadrotor UAV," in *2016 IEEE International Conference on Robotics and Automation (ICRA)*, May 2016, pp. 1492–1498.
- [4] J. T. Economou, G. Kladis, A. Tsourdos, and B. A. White, "UAV optimum energy assignment using dijkstra's algorithm," in *Control Conference (ECC), 2007 European*, July 2007, pp. 287–292.
- [5] N. Ure, G. Chowdhary, T. Toksoz, J. How, M. Vavrina, and J. Vian, "An automated battery management system to enable persistent missions with multiple aerial vehicles," *Mechatronics, IEEE/ASME Transactions on*, vol. 20, no. 1, pp. 275–286, Feb 2015.
- [6] J. Leonard, A. Savvaris, and A. Tsourdos, "Energy management in swarm of unmanned aerial vehicles," in *Unmanned Aircraft Systems (ICUAS), 2013 International Conference on*, May 2013, pp. 124–133.
- [7] A. Abdilla, A. Richards, and S. Burrow, "Power and endurance modelling of battery-powered rotorcraft," in *Intelligent Robots and Systems (IROS), 2015 IEEE/RSJ International Conference on*, Sept 2015, pp. 675–680.
- [8] T. Dietrich, O. Andryeyev, and A. Zimmermann, "Towards a unified decentralized swarm management and maintenance coordination based on mavlink," in *IEEE Int. Conf. on Autonomous Robot Systems and Competitions (ICARSC 2016)*, 05 2016.
- [9] "Solo - The Smart Drone," 3D Robotics - Drone & UAV technology, (visited on 05-Nov-2016). [Online]. Available: <https://3dr.com/solo-drone/>
- [10] "Copter Home," (visited on 05-Nov-2016). [Online]. Available: <http://ardupilot.org/copter/>
- [11] "Mission Planner Home," (visited on 05-Nov-2016). [Online]. Available: <http://ardupilot.org/planner/index.html>

$$Q_{pred} = \begin{cases} I_G \cdot t_c & \text{if } \vec{s} = \vec{0} \\ (I_G + I_M(\alpha_c)) \cdot d_c/v(\alpha_c) & \text{if } \vec{s} \neq \vec{0} \end{cases} \quad (4)$$

In case of a hover maneuver, the movement consumption $Q_M(\alpha, d_c)$ is equal to zero, because with $\vec{s} = \vec{0}$ the parameters α and d_c are undefined.

It should be noted that the electric current I and the electric charge Q are used as physical variables. They are proportional to electric power (respectively electric energy) and serve a better comparability with the battery capacity of multicopters, which is commonly specified in mA h.

D. Validation

In order to verify the accuracy of the energy consumption profile, we calculated prediction values for a third benchmark flight and compared the results with real-world flight measurements.

Table II shows the prediction results and the validation flight data for comparison. The prediction is represented by lower and upper bounds of 1σ deviation around the mean Q_{pred} .

The results in the table show, that the real-world measurements from the validation flight are in good proximity to our predicted energy consumption values. The difference stays within the 1σ bound, except for two outliers. The reason for these deviations and the outliers is suspected in the external influences, like wind, as mentioned in Section III.

The achieved prediction accuracy is sufficient for our future evaluation of fail-safe in-flight energy prediction.

TABLE II
ENERGY PREDICTION AND VERIFICATION

Command Parameters		Prediction Q_{pred}	Validation Flight	
Distance d_c	Angle α_c	Lower – Upper	Reading	Z-Score
Flight Part 1: Triangle				
74.29 m	15.6°	67.5–72.8 mA h	71.1 mA h	0.37
106.01 m	0°	55.8–67.6 mA h	65.3 mA h	0.62
74.29 m	–15.6°	86.9–96.9 mA h	88.9 mA h	–0.59
Flight Part 2: Rectangle				
70 m	90°	143.0–155.6 mA h	154.8 mA h	0.87
106.01 m	0°	55.8–67.6 mA h	68.0 mA h	1.07
70 m	–90°	172.4–187.4 mA h	178.9 mA h	–0.13
Flight Part 3: Zig-Zag				
82.59 m	57.9°	165.6–186.6 mA h	189.6 mA h	1.28
111.24 m	0°	58.6–71.0 mA h	68.0 mA h	0.52
70.15 m	–34.8°	128.5–146.4 mA h	134.2 mA h	–0.36
70.15 m	34.8°	117.8–123.5 mA h	122.0 mA h	0.47
111.24 m	0°	58.6–71.0 mA h	70.8 mA h	0.97
82.59 m	–57.9°	182.7–213.5 mA h	211.4 mA h	0.87
Σ		1293.2–1459.8 mA h	1423.3 mA h	